TIME-FREQUENCY REPRESENTATIONS WITH MULTIFORM, TILTABLE CHEBYSHEV KERNELS*

Antonio H. Costa [a] and *G. Faye Boudreaux-Bartels* [b]

a) Department of Electrical and Computer Engineering, University of Massachusetts Dartmouth
285 Old Westport Road, North Dartmouth, MA 02747-2300, USA
E-mail: acosta@umassd.edu

b) Department of Electrical Engineering, University of Rhode Island, Kingston, RI 02881-0805, USA
E-mail: boud@ele.uri.edu

ABSTRACT

In this paper, we formulate and provide design equations for novel time-frequency representations (TFRs) with multiform, tiltable (MT) Chebyshev kernels whose passband support regions are capable of attaining a wide diversity of iso-contour shapes in the ambiguity function (AF) plane, e.g., parallel strips, crosses, tilted and untilted ellipses, diamonds, hyperbolas, rectangles, etc. Simple constraints on the parameters of the new kernels can be used to guarantee many desirable properties of TFRs.

1. BACKGROUND

Quadratic TFRs of Cohen's shift-covariant class or the Hyperbolic Class can be characterized by a unique signal-independent kernel. They can give rise to cross terms which can cause serious interpretation problems. Since auto terms map to the origin of the AF plane whereas cross terms map away from the origin [1], the problematic cross terms can be reduced by letting the TFR's kernel be a two-dimensional lowpass filter in the AF plane.

None of the known lowpass kernels is ideal. Simple binary masks or "brick wall" kernels that are one in some regions of the AF plane and zero elsewhere can give rise to impulse responses that are infinite length and that exhibit a large amount of ringing in the time-frequency plane or in the temporal or spectral lag planes. The spectrogram suffers from a trade-off between time and frequency resolution. Other Cohen's class TFRs use kernels having passband support regions restricted to either hyperbolic (Choi-Williams distribution (CWD), generalized exponential distribution (GED), and Butterworth distribution (BUD) [1]), elliptic (tilted Gaussian distribution (TGD) [2]), or vertical and horizontal "strips" (smoothed pseudo Wigner distribution (SPWD) [1]) iso-contour shapes in the AF plane. Many existing TFRs are incapable of performing well for signal components that are closely spaced or that are linear FM chirps with different energy and sweep rate. The data-adaptive Gaussian kernel distribution [1] does well for linear FM chirps if they have equal energy.

2. MULTIFORM, TILTABLE TFRS

We extend the MT Gaussian and Butterworth TFRs in [3,4] to the MT Chebyshev distribution (MTCHED) with kernel

$$\Psi_{\mathrm{MTCHED}}(\tau,\nu)=\left\{1+K_p C_\lambda^2\left[\mu\left(\frac{\tau}{\tau_0},\frac{\nu}{\nu_0};\alpha,r,\beta,\gamma\right)\right]\right\}^{-1}, \quad (1)$$

and to the MT inverse Chebyshev distribution (MTICHED) with kernel

$$\Psi_{\mathrm{MTICHED}}(\tau,\nu)=\left\{1+K_s C_\lambda^{-2}\left[\mu^{-1}\left(\frac{\tau}{\tau_0},\frac{\nu}{\nu_0};\alpha,r,\beta,\gamma\right)\right]\right\}^{-1}, \quad (2)$$

where the nonlinear time-frequency mapping function $\mu(\cdot)$ is defined as [3,4]

$$\mu(\hat{\tau},\hat{\nu};\alpha,r,\beta,\gamma)=\hat{\tau}^2\left(\hat{\nu}^2\right)^{\alpha}+\left(\hat{\tau}^2\right)^{\alpha}\hat{\nu}^2+2r\left[\left(\hat{\tau}\hat{\nu}\right)^{\beta}\right]^{\gamma}. \quad (3)$$

The "design" parameters of these kernels are the powers $\alpha \geq 0$ and $\lambda > 0$, positive time-lag and frequency-lag scaling constants τ_0 and ν_0, respectively, a tilt parameter r, and the powers β and γ that are either $(\beta,\gamma) = (1,1)$ for causing no change, or $(\beta,\gamma) = (2,½)$ for producing the magnitude of the product term, $\hat{\tau}\hat{\nu}$. $C_\lambda(\cdot)$ is the Chebyshev polynomial of order λ. The passband region is assumed to have kernel values greater than or equal to k_p whereas the stopband region has kernel values less than or equal to k_s. $K_p=(1-k_p)/k_p$ and $K_s=(1-k_s)/k_s$.

The first advantage of the proposed kernels is their ability to generate arbitrarily narrow transition regions and a wider variety of passband/stopband support regions in the AF plane than conventional Cohen's class kernels by properly choosing combinations of the kernel parameters, e.g., *parallel strips* at arbitrary angles ($0 \leq \alpha \leq 0.001$, $r = \pm 1$, $\beta = \gamma = 1$), *crosses* ($0 \leq \alpha \leq 0.001$, $r = -1$, $\beta = 2$, $\gamma = ½$), "*snowflakes*" ($0 \leq \alpha \leq 0.001$, $r < -1$, $\beta = 2$, $\gamma = ½$), *untilted ellipses* ($0 \leq \alpha \leq 0.01$, $r = 0$), *tilted ellipses* ($0 \leq \alpha \leq 0.01$, $-1 < r < 1$, $\beta = \gamma = 1$), *diamonds* ($0 \leq \alpha \leq 0.1$, $r = 1$, $\beta = 2$, $\gamma = ½$), *hyperbolas*

* Work supported in part by ONR grant N00014-92-J-1499.

0-7803-2431-5/95 $4.00

($\frac{1}{4} < \alpha < 2.5, r = 0$), *rectangles* ($\alpha \to \infty$, $r = 0$), etc. See Figs. 1-2. This versatility enables the new kernels to suppress undesirable cross terms in a broader variety of time-frequency scenarios. For example, a simulation involving the sum of four complex chirps having unequal chirp rates, depicted in Fig. 3, makes conventional kernel design difficult. Fig. 3(a) displays the Wigner distribution (WD) of the composite signal whereas Fig. 3(b) shows the MTCHED result computed using a "snowflake" kernel. Fig. 3(c) depicts the CWD result and Fig. 3(d) shows the cone kernel distribution (CKD) [1] when a 51-point Hamming window is used. Since the lowest amplitude contour level plotted is one tenth that of the maximum, the cross terms remaining in the CWD and CKD are non-trivial. The TGD also performs poorly when chirp signals with different chirp rates are present. As another example, Fig. 5 shows a spectrogram and MTCHED of real speech data. The MTCHED in Fig. 5(c) clearly depicts the three formant frequencies and the broadband impulsive character at the onset of each pitch period.

The second advantage is that we derive closed form design equations to select kernel parameters that meet or exceed the given user specified passband and stopband design criteria in the AF plane. Most Cohen's class TFRs have only ad-hoc techniques for parameter selection. Further, MT TFRs have arbitrarily narrow transition regions that can satisfy both passband and stopband constraints simultaneously; the CWD and the TGD cannot. Of all the MT kernels that meet user specifications, the one with the widest transition region is chosen to minimize the effective length and the amount of ringing in the kernel's impulse response [5].

Thirdly, simple constraints on the parameters of the new kernels can be used to guarantee many desirable properties of TFRs. For example, the only requirement needed to satisfy the TFR marginal properties and moment properties [1,3,4] is that the parameter α in (1)-(3) be non-zero (and λ odd for the MTCHED). Since α is non-zero in Fig. 3(b), the TFRs in Figs. 3(a)-(c) satisfy the marginal properties, but the MTCHED is the most effective at cross term reduction and auto term preservation.

3. MTCHED PARAMETER DESIGN

We outline a design algorithm which uses the location of the auto terms and cross terms in the AF plane to derive the kernel parameters for the case of diamond shaped contours of the MTCHED kernel. The algorithm assumes that we are given k_p, k_s, and a set of $N_p \geq 2$ passband points, $\left\{\left(\tau_{p_i}, \nu_{p_i}\right)\right\}_{i=1}^{N_p}$, which must lie in the passband, i.e., it is desired that $\Psi_{\text{MTCHED}}\left(\tau_{p_i}, \nu_{p_i}\right) \geq k_p$, and a set of $N_s \geq 1$ stopband points, $\left\{\left(\tau_{s_i}, \nu_{s_i}\right)\right\}_{i=1}^{N_s}$, i.e., it is desired that $\Psi_{\text{MTCHED}}\left(\tau_{s_i}, \nu_{s_i}\right) \leq k_s$. See Fig. 4.

By constraining $0 \leq \alpha \leq 0.1$, $r = +1$, $\beta = 2$, and $\gamma = \frac{1}{2}$ in (1), the MTCHED generates kernels whose passband support is bounded by a diamond in the AF plane. Moreover, when $\alpha = 0$ in (1), the passband MTCHED kernel iso-contour, $\Psi_{\text{MTCHED}}(\tau,\nu) = k_p$, occurs at

$$|\tau| / \tau_0 + |\nu| / \nu_0 = 1. \tag{4}$$

Because of the symmetry present in this analysis, we can restrict the parameter design analysis to the first quadrant of the AF plane, in which case (4) can be rewritten as

$$\nu = m_p \tau + b_p \tag{5}$$

with the slope parameter

$$m_p = -\nu_0 / \tau_0 \tag{6}$$

and the "ν-intercept" (passband) parameter

$$b_p = \nu_0 \tag{7}$$

which are dependent upon the unknown MTCHED kernel parameters ν_0 and τ_0. Similarly, the stopband MTCHED kernel iso-contour, $\Psi_{\text{MTCHED}}(\tau,\nu) = k_s$, is

$$\nu = m_p \tau + b_s \tag{8}$$

with the same slope, m_p, in (6) but different (stopband) ν-intercept

$$b_s = \nu_0 \sqrt{\cosh\left\{\lambda^{-1} \operatorname{arccosh}\left[\sqrt{\left[(1-k_s)k_p\right] / \left[(1-k_p)k_s\right]}\right]\right\}}. \tag{9}$$

The MTCHED kernel design algorithm finds an outermost diamond shaped boundary for the given passband points and a concentric, innermost diamond shaped boundary for the stopband points (see Fig. 4), and then uses the intercepts (b_p and b_s) and equal slope (m_p) of these two diamonds to solve for the unknown MTCHED parameters λ, ν_0, and τ_0 in (6), (7) and (9).

The outermost "passband" diamond is found by using each pair of the given passband points $\left\{\left(\tau_{p_i}, \nu_{p_i}\right)\right\}_{i=1}^{N_p}$ to define a line. A search is made for the critical passband line, which is the outermost one that has all passband points below it or on it, i.e.,

$$\nu_{p_i} \leq m_p \tau_{p_i} + b_p \quad , i = 1,2,\cdots,N_p. \tag{10}$$

If $\left(\tau_{cp_1}, \nu_{cp_1}\right)$ and $\left(\tau_{cp_2}, \nu_{cp_2}\right)$ are the pair of passband points that generated the critical passband line[1] in (10), then its slope and ν-intercept are, respectively,

[1] When multiple "critical" passband lines occur, a search is made for the pair of parallel passband and stopband lines which provide the smallest order parameter λ, to minimize the chance of overflow problems in the computation of the kernel and to produce the widest possible transition region [3,4].

$$m_p = \left(\nu_{cp_2} - \nu_{cp_1}\right) / \left(\tau_{cp_2} - \tau_{cp_1}\right) \quad (11)$$

and $$b_p = \nu_{cp_1} - m_p \tau_{cp_1}. \quad (12)$$

Similarly, the innermost "stopband" line is found by using each stopband point $\left\{\left(\tau_{s_i}, \nu_{s_i}\right)\right\}_{i=1}^{N_s}$ and the slope, m_p, found in (11) to define a line. The critical stopband line is the innermost one that has all stopband points above it or on it, i.e.,

$$\nu_{s_i} \geq m_p \tau_{s_i} + b_s \quad , i = 1,2,\cdots,N_s. \quad (13)$$

Let (τ_{cs}, ν_{cs}) be the stopband point that generated the critical stopband line in (13). Then, the ν-intercept of this (parallel) stopband critical line is

$$b_s = \nu_{cs} - m_p \tau_{cs}. \quad (14)$$

Given m_p, b_p, and b_s in (11), (12), and (14), the order parameter λ can be found by first simplifying the ratio of b_p and b_s in (7) and (9); ν_0 and τ_0 are found using (6) and (7). Tables 1 and 2 summarize the design equations for the diamond shaped contour in (4) as well as other possible shapes of passband/stopband support regions for the MT Chebyshev and inverse Chebyshev kernels [3].

The procedure described above assumed that $\alpha = 0$. However, increasing α slightly, produces TFRs that satisfy both the desirable marginal properties of TFRs [1] and produce the desired diamond shaped passband iso-contours in the AF plane, except very near the τ-ν axes.

4. CONCLUSIONS

We have proposed versatile, Chebyshev kernels for TFRs capable of attaining many possible passband support shapes with arbitrarily narrow transition regions in the AF plane. The most useful shapes are: ellipses (tilted and untilted), parallel strips, crosses, diamonds, hyperbolas, "snowflakes", and rectangles. For given passband and stopband constraints, we developed simple and fast design equations for the kernel parameters that meet or exceed user specified criteria. Simulations reveal that the MT TFRs are capable of outperforming classical Cohen's class TFRs in many situations. The main disadvantage is that the user must specify the boundary between the auto and cross terms in the AF plane.

REFERENCES

[1] F. Hlawatsch and G. F. Boudreaux-Bartels, "Linear and quadratic time-frequency signal representations," *IEEE Signal Processing Magazine*, vol. 9, pp. 21-67, Apr. 1992.

[2] A. H. Nuttall, "Alias-free smoothed Wigner distribution function for discrete-time samples," NUSC, New London, CT, *Technical Report 8785*, October 1990.

[3] A. H. Costa, *Multiform, Tiltable Time-Frequency Representations and Masked Auto Wigner Distribution Synthesis*. Ph.D. dissertation, University of Rhode Island, Kingston, RI, 1994.

[4] A. H. Costa and G. F. Boudreaux-Bartels, "Design of time-frequency representations using multiform, tiltable kernels," *Proc. of the IEEE-SP International Symposium on Time-Frequency and Time-Scale Analysis*, pp. 205-208, 1994.

[5] L. B. Jackson, *Digital Filters and Signal Processing*. Boston, MA: Kluwer Academic Publishers, 1989.

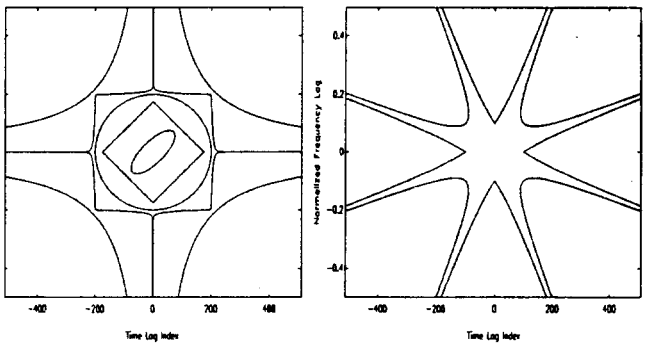

(a) (b)

Figure 1: 50% iso-contours in the AF plane demonstrating some of the possible passband support regions (hyperbolic, rectangular, elliptical, diamond, and "tilted ellipse" in (a) and "snowflake" in (b)) for the MT Chebyshev kernels.

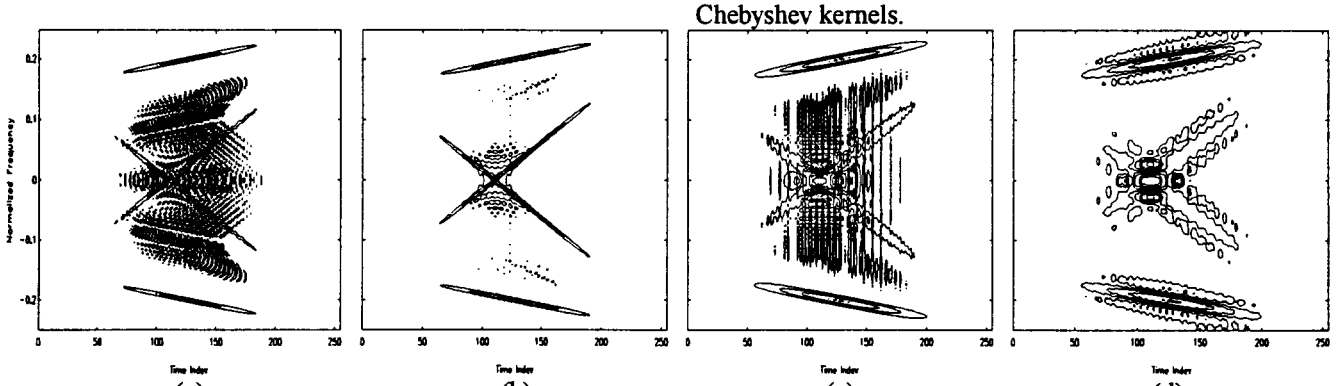

(a) (b) (c) (d)

Figure 3: Contour plots for four complex chirps with unequal chirp rates. (a) WD; (b) MTCHED with a "snowflake" kernel; (c) CWD with $\sigma = 50$; (d) cone kernel distribution (CKD) when a 51-point Hamming window is used. Twelve linearly spaced contours between $-\xi$ to -0.1ξ and 0.1ξ to ξ are displayed, where ξ is the maximum magnitude of the TFR.

MT TFR Form	*Intermediate Design Parameters*				*Constraints*			
	m_p	m_s	b_p	b_s	α	r	β	γ
Untilted Ellipse	$\frac{\nu_{cp_2}^2 - \nu_{cp_1}^2}{\tau_{cp_2}^2 - \tau_{cp_1}^2}$		$\nu_{cp_1}^2 - m_p\tau_{cp_1}^2$	$\nu_{cs}^2 - m_p\tau_{cs}^2$	0	0		
Parallel Strip Cross Diamond	$\frac{\nu_{cp_2} - \nu_{cp_1}}{\tau_{cp_2} - \tau_{cp_1}}$		$\nu_{cp_1} - m_p\tau_{cp_1}$	$\nu_{cs} - m_p\tau_{cs}$	0	± 1 -1 $+1$	1 2 2	1 ½ ½
Hyperbola	$\tau_{cp_1}\nu_{cp_1}$	$\tau_{cs}\nu_{cs}$			1	0		

Table 1: Design equations for the intermediate parameters of the MT TFRs. $(\tau_{cp_i}, \nu_{cp_i})$, $i = 1,2$ are the passband points defining the critical passband curve while (τ_{cs}, ν_{cs}) is the stopband point defining the critical stopband curve.

	Multiform, Tiltable (MT) TFR Design Parameters		
MT TFR Form	λ	ν_0	τ_0
Untilted Ellipse: MTCHED	$\cosh^{-1}\left(\sqrt{K_s/K_p}\right)/\cosh^{-1}\left[(b_s/b_p)\right]$	$\sqrt{b_p}$	$\frac{\nu_0}{\sqrt{-m_p}}$
MTICHED		$\sqrt{b_s}$	
Parallel Strip, Cross, Diamond: MTCHED	$\cosh^{-1}\left(\sqrt{K_s/K_p}\right)/\cosh^{-1}\left[(b_s/b_p)^2\right]$	b_p	$\frac{-r\nu_0}{m_p}$
MTICHED		b_s	
Hyperbola: MTCHED	$\cosh^{-1}\left(\sqrt{K_s/K_p}\right)/\cosh^{-1}\left[(m_s/m_p)^2\right]$	$\tau_0\nu_0 = \sqrt{2}m_p$	
MTICHED		$\tau_0\nu_0 = \sqrt{2}m_s$	

Table 2: Design equations for the parameters of the MT kernels in (1)-(2) using m_p, m_s, b_p, b_s, α, r, β, and γ listed in Table 1. $K_p = (1-k_p)/k_p$, $K_s = (1-k_s)/k_s$, where k_p is the minimum passband amplitude and k_s is the maximum stopband amplitude.

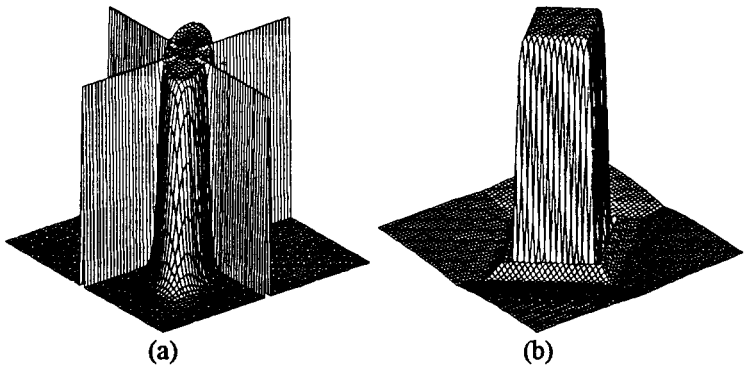

(a) (b)

Figure 2: (a) Mesh plot of the MTCHED kernel ("tilted ellipse", $\lambda = 3$) illustrating the passband ripple. Notice that since $\alpha = 0.001$ and λ is odd, the kernel is equal to one along the axes of the AF plane and, hence, the TFR marginal properties are satisfied. (b) Mesh plot of the MTICHED kernel ("diamond", $\lambda = 4$) illustrating the stopband ripple.

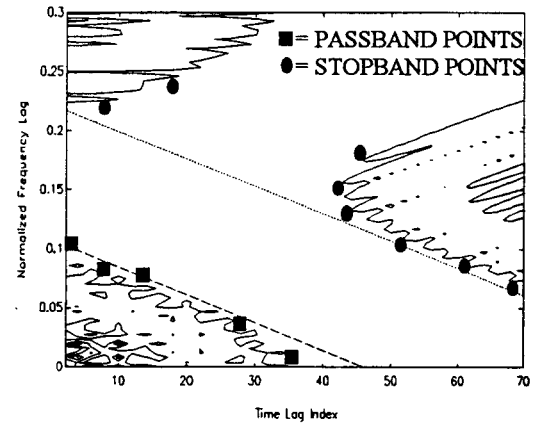

Figure 4: Diagram of the AF plane showing the selected passband points, stopband points, and the associated critical passband line (dashed) and critical stopband line (dotted). A partial contour plot of the AF of a signal is also shown (solid lines), with passband points chosen around the edge of the auto terms and stopband points chosen around the closest cross terms.

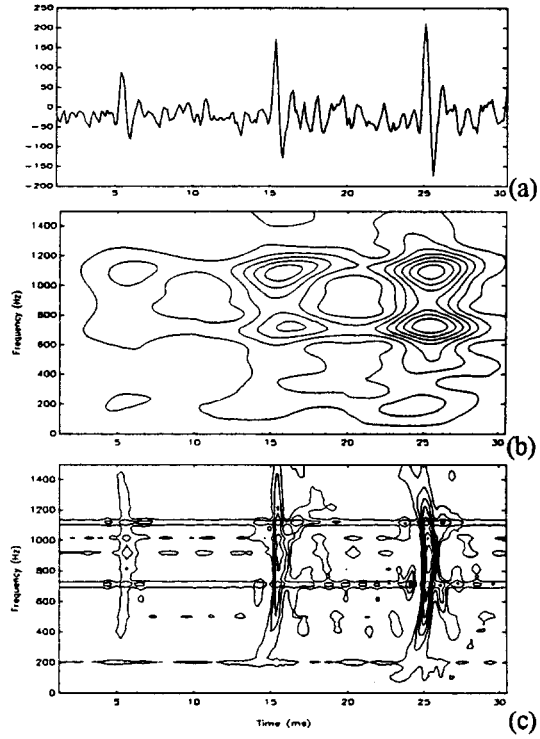

Figure 5: Time-frequency analysis of the phoneme "ah" spoken by a male speaker. The sampling rate is 8000 Hz. (a) Time series for three pitch periods; (b) spectrogram with a 10-ms Hamming window; (c) MTCHED with $\tau_0 = 23.7831$, $\nu_0 = 0.1627$, $r = 0$, $\alpha = 0.001$, and $\lambda = 4.2236$. The linearly spaced contours in (b)-(c) span two orders of magnitude.